Editors' Suggestion

Improved search for heavy neutrinos in the decay $\pi \to e\nu$

A. Aguilar-Arevalo,[1] M. Aoki,[2] M. Blecher,[3] D. I. Britton,[4] D. vom Bruch,[5,†] D. A. Bryman,[5,6] S. Chen,[7] J. Comfort,[8] S. Cuen-Rochin,[5] L. Doria,[6,9,*] P. Gumplinger,[6] A. Hussein,[6,10] Y. Igarashi,[11] S. Ito,[2,‡] S. Kettell,[12] L. Kurchaninov,[6] L. S. Littenberg,[12] C. Malbrunot,[5,§] R. E. Mischke,[6] T. Numao,[6] D. Protopopescu,[4] A. Sher,[6] T. Sullivan,[5,‖] and D. Vavilov[6]

(PIENU Collaboration)

[1]*Instituto de Ciencias Nucleares, Universidad Nacional Autónoma de México, CDMX 04510, México*
[2]*Physics Department, Osaka University, Toyonaka, Osaka 560-0043, Japan*
[3]*Virginia Tech., Blacksburg, Virginia 24061, USA*
[4]*SUPA—School of Physics and Astronomy, University of Glasgow, Glasgow G12 8QQ, United Kingdom*
[5]*Department of Physics and Astronomy, University of British Columbia, Vancouver, British Columbia V6T 1Z1, Canada*
[6]*TRIUMF, 4004 Wesbrook Mall, Vancouver, British Columbia V6T 2A3, Canada*
[7]*Department of Engineering Physics, Tsinghua University, Beijing 100084, China*
[8]*Physics Department, Arizona State University, Tempe, Arizona 85287, USA*
[9]*Institut für Kernphysik, Johannes Gutenberg-Universität Mainz, Johann-Joachim-Becher-Weg 45, D 55128 Mainz, Germany*
[10]*University of Northern British Columbia, Prince George, British Columbia V2N 4Z9, Canada*
[11]*KEK, 1-1 Oho, Tsukuba-shi, Ibaraki 305-0801, Japan*
[12]*Brookhaven National Laboratory, Upton, New York 11973-5000, USA*

(Received 8 December 2017; published 17 April 2018)

A search for massive neutrinos has been made in the decay $\pi^+ \to e^+\nu$. No evidence was found for extra peaks in the positron energy spectrum indicative of pion decays involving massive neutrinos ($\pi \to e^+\nu_h$). Upper limits (90% C.L.) on the neutrino mixing matrix element $|U_{ei}|^2$ in the neutrino mass region 60–135 MeV/c^2 were set and are an order of magnitude improvement over previous results.

DOI: 10.1103/PhysRevD.97.072012

I. INTRODUCTION

In the original Standard Model (SM) [1], neutrinos are included as massless particles. There is now firm experimental evidence that neutrinos oscillate between different flavors, indicating that at least two are massive particles [2].

Many extensions of the SM incorporating massive neutrinos hypothesize the existence of additional neutrino states. Right-handed gauge singlets (sterile neutrinos) are an essential ingredient in seesaw models [3] aiming to explain the smallness of neutrino masses. In the neutrino minimal Standard Model [4] (νMSM), three sterile neutrinos and three corresponding mass eigenstates are added, leading to new mixings between six definite mass states and the active and sterile states. For example, depending on the choices of parameters and mass hierarchy in the νMSM, the two heaviest sterile neutrino states may occur in the range probed by meson decays [5], while the lightest state can play a role as a dark matter particle in the keV/c^2 mass range. Massive neutrinos in the MeV/c^2 range are also required in dark matter models addressing small scale structure problems [6] or involving new thermalization scenarios [7]. More generally, for k sterile neutrinos, the weak eigenstates ν_{χ_k} are related to the mass eigenstates ν_i by a unitary transformation matrix $U_{\ell i}$, where $\nu_\ell = \Sigma_{i=1}^{3+k} U_{\ell i}\nu_i$, with $\ell = e, \mu, \tau, \chi_1, \chi_2 \ldots \chi_k$.

*Corresponding author.
luca@triumf.ca, doria@uni-mainz.de
†Present address: LPNHE, Sorbonne Université, Université Paris Diderot, CNRS/IN2P3, Paris, France.
‡Present address: Faculty of Science, Okayama University, Okayama, 700-8530, Japan.
§Present address: Experimental Physics Department, CERN, Genève 23, CH-1211, Switzerland.
‖Present address: Department of Physics, Queen's University, Kingston K7L 3N6, Canada.

Depending on the mass scale of the new heavy mass eigenstates, sterile neutrinos can have different phenomenological signatures. If heavy neutrino states are Majorana fermions, neutrinoless double beta decay experiments may provide stringent constraints [8]. Other constraints on $U_{\ell i}$ come from lepton universality tests, the decay width of invisible decays of Z bosons, μ and τ lepton-flavor-violating decays, and magnetic and electric dipole moments of charged leptons [8]. In particular, heavy neutrinos with MeV/c^2 to GeV/c^2 masses can have measurable effects in meson decays that can be explored by precisely measuring their decay branching ratios or by searching for extra peaks in the energy spectrum of their leptonic two-body decays (e.g. $\pi, K, B \to l\nu$) [9].

The decay $\pi^+ \to e^+\nu$ (positron energy $E_{e^+} = 69.8$ MeV) is helicity suppressed in the SM, and its measured branching ratio is $R_{\rm exp} = (1.2327 \pm 0.0023) \times 10^{-4}$ [10–13]. The presence of heavy neutrinos relaxes the helicity suppression; comparing the experimental value with the theoretical SM calculation $R_{\rm SM} = (1.2352 \pm 0.0002) \times 10^{-4}$ [14–16], limits on $|U_{ei}|^2$ have been obtained for masses below 60 MeV/c^2 [13]. Previous searches for additional peaks in $\pi^+ \to e^+\nu$ decays [17,18] established upper limits at the level of $|U_{ei}|^2 < 10^{-7}$ in the neutrino mass region of 50–130 MeV/c^2 and were limited by the presence of the $\mu^+ \to e^+\nu\bar{\nu}$ decay background ($E_{e^+} = 0.5$–52.8 MeV) originating from decays in flight of pions. An improved limit was published in Ref. [19] based on a partial data set from the PIENU experiment.

In the present work, we present a search for additional peaks in the low-energy region of the background-suppressed $\pi^+ \to e^+\nu$ spectrum using the full data set collected by the PIENU experiment, representing a sample larger than [19] by an order of magnitude.

II. EXPERIMENTAL TECHNIQUE

The π^+ beam was provided by the TRIUMF M13 beam line, modified to deliver 75 ± 1 MeV/c pions with $< 2\%$ positron contamination [20]. A detailed description of the PIENU detector (Fig. 1) can be found in Ref. [21]. Briefly, beam tracking was realized by two sets of multiwire proportional chambers (WC1 and 2), each with three planes of wires oriented at 60° to each other. After WC1/2, the beam was degraded by two plastic scintillators (B1 and B2). These provided the pion-arrival trigger signal, energy loss measurement for particle identification, and detection of extra beam particles. Pions were stopped in an 8 mm thick plastic scintillator (B3) where they decayed at rest via $\pi^+ \to e^+\nu$ or $\pi^+ \to \mu^+ \to e^+$ ($\pi^+ \to \mu^+\nu$ followed by $\mu^+ \to e^+\nu\bar{\nu}$). Two sets of silicon microstrip detectors (S1 and S2), each with two orthogonal planes, were installed upstream of B3 for tracking pions and (together with the pion track information from WC1/2) to detect decays in flight. After B3, a third silicon microstrip detector (S3) and a wire chamber (WC3) provided tracking for decay positrons.

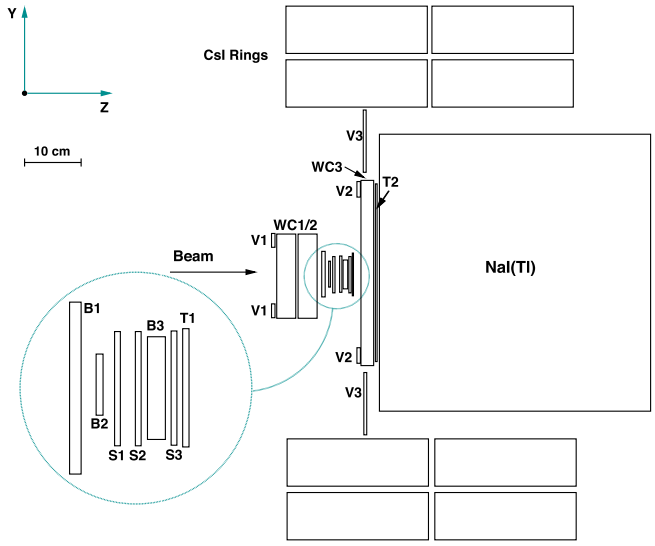

FIG. 1. Schematic illustration of the PIENU detectors with the pion stopping region shown in the inset.

Two plastic scintillators (T1 and T2) provided the decay trigger signal. WC3 and T2 were mounted in front of a NaI($T\ell$) calorimeter crystal (a 48 cm diameter × 48 cm long cylinder), which provided the main positron energy measurement. The NaI($T\ell$) calorimeter was surrounded by 97 pure CsI crystals arranged in a two-layer concentric structure for electromagnetic shower leakage detection. The trigger logic was based on a pion signal provided by the coincidence B1·B2·B3 (with a high B1 threshold to select pions) and a decay-positron signal provided by a T1·T2 coincidence. A coincidence of pion-arrival and decay-positron signals within a time window from −300 to 540 ns defined the logic for an unbiased collection of events, prescaled by a factor 16. Another trigger was based on a decay-positron signal in the 2 to 40 ns time window without prescaling, containing most of the $\pi^+ \to e^+\nu$ events. Continuous calibration of the detectors was provided by dedicated beam-positron and cosmic-ray triggers. The typical pion stopping rate was 5×10^4 s^{-1}, while the trigger rate was 600 s^{-1}. Plastic scintillators, and NaI(Tl) and CsI calorimeters were read out by waveform digitizers at 500, 30, and 60 MHz respectively. Silicon detectors were digitized at 60 MHz, while the wire chambers and trigger signals were read by multihit time-to-digital converters with 0.625 ns resolution.

III. DATA ANALYSIS

A. Event selection

The analysis included four data sets with approximately 10^7 $\pi^+ \to e^+\nu$ events collected over a period of four years, including the data used in the previous search [19] based on 10^6 $\pi^+ \to e^+\nu$ events. Automatic calibration procedures

and run-by-run gain stability corrections of the detectors ensured similar decay spectra for all data sets. The event selection adopted the same strategy as for the extraction of the $\pi^+ \to e^+\nu$ branching ratio [13]. Pions were identified based on their energy loss in B1 and B2, and a cut was applied to WC1/2 to exclude beam halo particles. Cuts based on waveform information from B1, B2, and T1 were used to reject events with additional beam particles. A fiducial radial cut of 80 mm in WC3 was used, resulting in 20% solid angle acceptance for positron tracks. A requirement of <2 MeV measured by the CsI array was applied to select events which were mainly contained in the higher resolution NaI($T\ell$) detector.

Suppression of $\pi^+ \to \mu^+ \to e^+$ events was based on timing, energy, and tracking information. Events in the 4–35 ns timing window were selected. The strongest suppression factor was given by the sum E_s of the energy deposits in B1, B2, S1, S2, and B3 (with a 100 ns integration window). For $\pi^+ \to \mu^+ \to e^+$ decay, the energy deposit in B3 was generally larger than for $\pi^+ \to e^+\nu$ decay by 4.1 MeV, due to the presence of the muon. However, due to the 100 ns integration window, which might miss the positron and light output saturation effects in the plastic scintillator, the energy distribution observed in B3 for $\pi^+ \to \mu^+ \to e^+$ events overlapped that for $\pi^+ \to e^+\nu$ events. Therefore, a cut in E_s with a width of 1 MeV was applied, as indicated in Fig. 2(a), to minimize the $\pi^+ \to \mu^+ \to e^+$ background.

The beam tracking detectors WC1/2 and $S1/2$ allowed the measurement of the vertex of pion decays in flight before B3 and, when combined with positron tracking information from S3 and WC3 downstream of B3, allowed an estimate of the decay vertex in the beam direction (Z); this latter distribution is broader in the case of $\pi^+ \to \mu^+ \to e^+$ events due to the distance traveled by the muon in B3. Cuts on the pion decay-in-flight track angle upstream of B3 [19] and Z vertex distributions [Fig. 2(b)] helped in rejecting the $\pi^+ \to \mu^+ \to e^+$ backgrounds.

The suppression cuts were optimized to minimize the figure of merit $\sqrt{N_L}/N_H$, where N_L and N_H are the numbers of events below and above 52 MeV in the positron energy spectrum. The cuts suppressed the backgrounds by a factor of 10^7 with the final positron energy spectrum, yielding $\sqrt{N_L}/N_H = 2.8 \times 10^{-4}$. The background-suppressed spectrum is shown in Fig. 3, where the majority of events are of the $\pi^+ \to e^+\nu$ type concentrated at the peak at 69.8 MeV with a low-energy tail extending below the background events (mainly $\pi^+ \to \mu^+ \to e^+$ where the pion or the muon decayed in flight near or in B3). The shoulder at about 58 MeV is due to photonuclear reactions in the NaI($T\ell$) followed by neutron emission and escape from the crystal [22].

B. Positron spectrum fit

The background-suppressed positron spectrum was used to search for additional peaks due to massive neutrinos. The spectrum was fitted from $E_{e^+} = 4$ MeV to $E_{e^+} = 56$ MeV with background components and a signal component. The lower limit of the fit was set by the lack of statistics and the sharp drop of the cut efficiencies, while the upper limit was set for avoiding the peaks due to photonuclear interactions. The fit was repeated, shifting the signal component in 0.25 MeV steps within the fitting range. The signal shape was simulated for every energy step with a Monte Carlo (MC) simulation validated with an experimental study of the calorimeter response to positrons. The shapes of the background components were obtained from late-time positrons ($t > 200$ ns) representing the $\pi^+ \to \mu^+ \to e^+$ decay chain, a component derived from MC describing $\pi^+ \to \mu^+ \to e^+$ events where the muon decayed in flight in B3, mimicking the $\pi^+ \to e^+\nu$ timing, and a $\pi^+ \to e^+\nu$ low-energy tail component due to electromagnetic shower losses, which was a triple-exponential fit to the MC spectrum. The fitted components are shown in Fig. 3. The background-only fit described the data well, yielding $\chi^2/\text{dof} = 197.2/203 = 0.97$, and the addition of purported

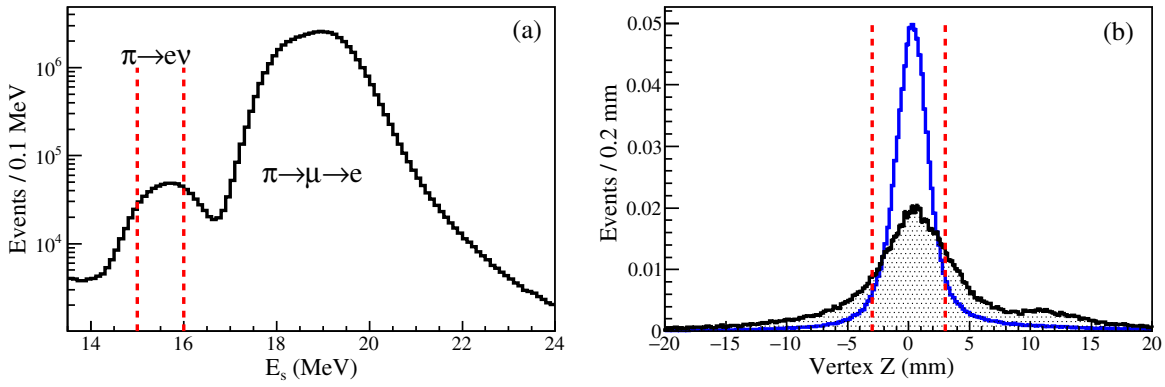

FIG. 2. (a) Energy sum E_s measured in B1, B2, S1, S2, and B3. (b) Z vertex for events with positron energy $E_{e^+} < 52$ MeV (shaded histogram) and $E_{e^+} > 52$ MeV (blue full line). The two distributions are normalized to contain the same number of events, and cuts applied are indicated by the red vertical dashed lines.

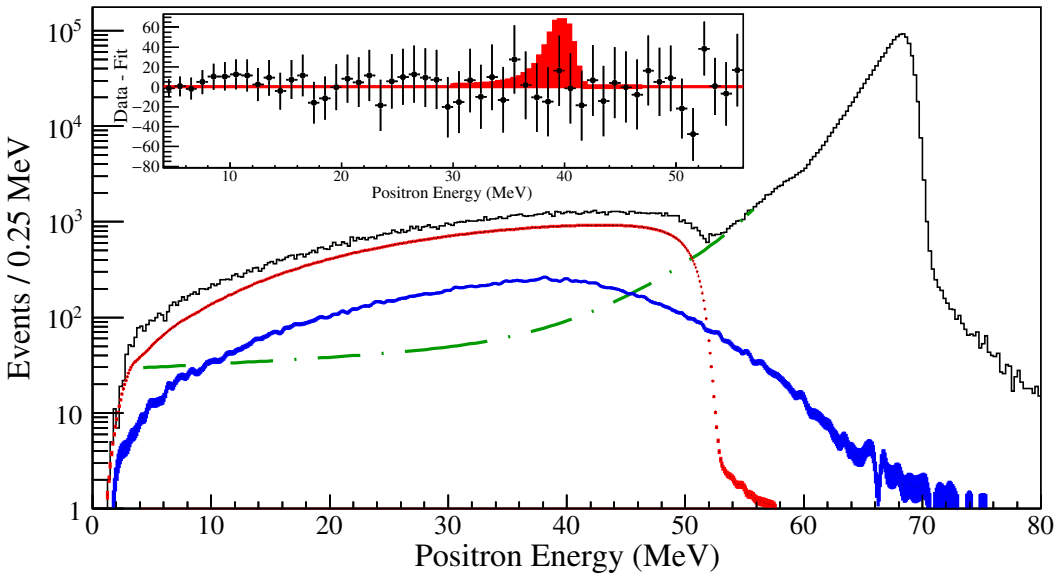

FIG. 3. Background-suppressed positron energy spectrum (black histogram). Fitted components include muon decays in flight (thick blue line, from MC), $\pi^+ \to e^+\nu$ (green, dot-dashed line, fit to MC), and $\pi^+ \to \mu^+ \to e^+$ (red dashed line, from late-time data events). The insert shows the (rebinned) residuals (Data–Fit) with statistical error bars and the signal shape in the case of $E_{e^+} = 40$ MeV and $|U_{ei}|^2 = 10^{-8}$.

signals did not change the result. Since no significant excesses beyond statistical fluctuations were found, upper limits $|U_{ei}|^2_{UL}$ on the couplings could be calculated.

C. Acceptance correction

Most systematic and acceptance effects canceled to first order, since the upper limit was proportional to the ratio of the fitted number of signal events and the number of $\pi^+ \to e^+\nu$ events $N(\pi \to e\nu_e)$, which were estimated by fitting a MC generated spectrum to the data for $E_{e^+} > 52$ MeV. However, energy-dependent effects induced by the suppression cuts did not completely cancel, and a correction was needed. The positron energy-dependent acceptance correction $\mathrm{Acc}(E_{e^+})$ was calculated via a MC simulation. Uniformly distributed positron tracks were simulated at a given energy E_{e^+} between 0 and 70 MeV in 0.25 MeV steps with the suppression cuts: energy sum E_s, Z vertex, and CsI veto. The ratio between the number of events at a given E_{e^+} and the number of events at $E_{e^+} = 70$ MeV was taken as the relative acceptance correction. The correction as a function of the positron energy is shown in Fig. 4. The statistical uncertainty due to the MC procedure is about 1%. The increase of the acceptance correction toward low energies is due to the CsI veto cut, which removes more high-energy events having larger shower leakage from the NaI(Tl) calorimeter. In order to estimate the systematic uncertainty on the acceptance correction, a study was performed using $\pi^+ \to \mu^+ \to e^+$ events. In contrast to $\pi^+ \to e^+\nu$ events, the background contribution to this spectrum was negligible; it had higher statistics and covered a broad energy range. Comparing $\pi^+ \to \mu^+ \to e^+$ events to the MC, the effect of the suppression cuts was studied, and good agreement with the data was found. The maximum difference between data and MC for $E_{e^+} > 10$ MeV was 3%, which was conservatively assigned to be the systematic uncertainty on the acceptance correction.

IV. RESULTS

Since no significant peaks were found in the data, 90% C.L. upper limits $N(\pi \to e\nu_i)_{UL}$ were calculated with a Bayesian procedure, assuming a flat prior and enforcing a positive peak amplitude and a Gaussian probability distribution.

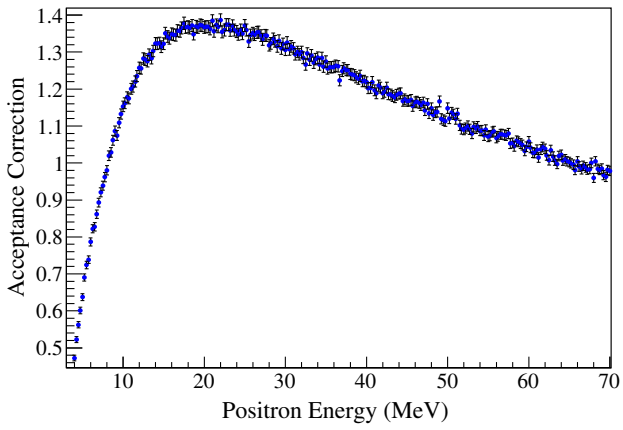

FIG. 4. Acceptance correction $\mathrm{Acc}(E_{e^+})$ as a function of the positron energy as determined with the MC simulation. The error bars are statistical only.

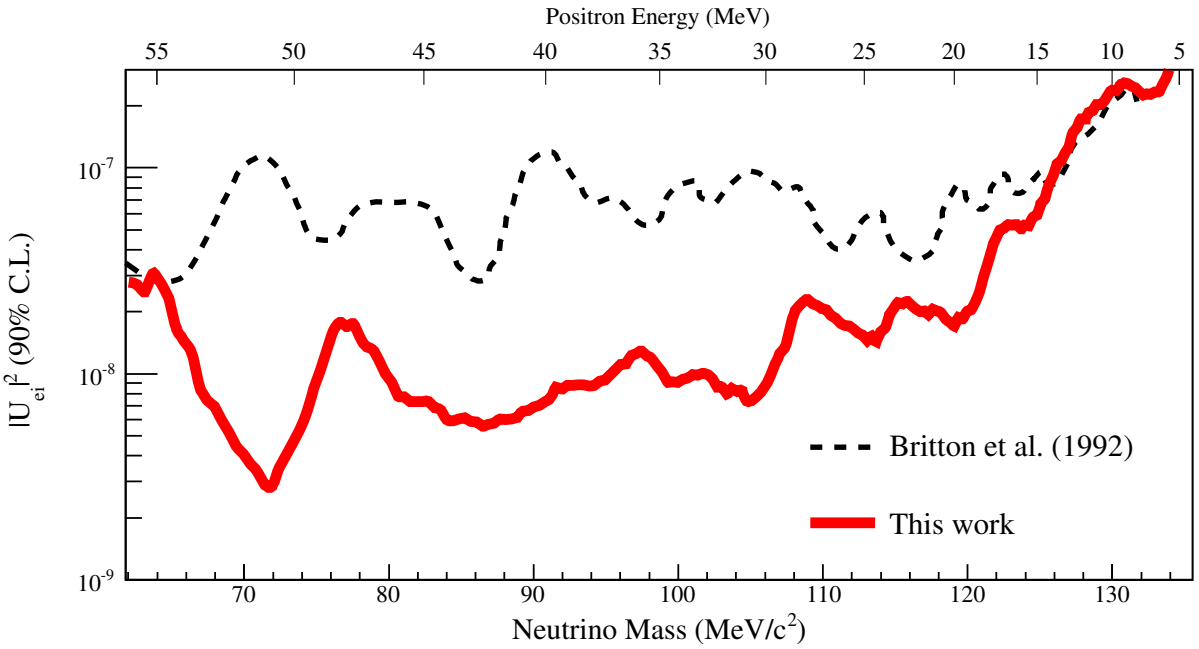

FIG. 5. 90% C.L. upper limits on the square of the mixing matrix elements $|U_{ei}|^2$ of heavy neutrinos coupled to electrons (thick red line). The black dashed line shows the results from Ref. [18].

An upper limit $|U_{ei}|^2_{UL}$ on the squared matrix element describing the mixing of the massive states with the other active neutrino states was obtained using

$$\frac{1}{\mathrm{Acc}(E_{e^+})}\frac{N(\pi \to e\nu_i)_{UL}}{N(\pi \to e\nu)} = |U_{ei}|^2_{UL}\rho_e(E_{e^+}), \qquad (1)$$

where $\rho_e(E_{e^+})$ is a phase space and helicity-suppression factor [9],

$$\rho_e(E_{e^+}) = \frac{\sqrt{1+\delta_e^2+\delta_i^2-2(\delta_e+\delta_i+\delta_e\delta_i)}}{\delta_e(1-\delta_e)^2} \times (\delta_e+\delta_i-(\delta_e-\delta_i)^2), \qquad (2)$$

where

$$\delta_e = m_e/m_\pi, \qquad \delta_i = m_{\nu_i}/m_\pi, \quad \text{and}$$
$$m_{\nu_i} = \sqrt{m_\pi^2 - 2m_\pi E_{e^+} + m_e^2}.$$

The results for the 90% C.L. upper limits for $|U_{ei}|^2$ [23] are shown in Fig. 5 (thick red line), together with the previous result [18] (black dashed line). These results supersede those reported in Ref. [19].

V. SUMMARY

A search has been performed for the mixing of heavy neutrinos coupled to electrons in the decay $\pi^+ \to e^+\nu_h$. No extra peaks due to heavy neutrinos were found in the positron energy spectrum, resulting in upper limits set on the square of the mixing matrix elements $|U_{ei}|^2$ from 10^{-8} to 10^{-7} for neutrino masses in the range 60–135 MeV/c^2. These results are independent of assumptions about the nature of the heavy neutrino and are comparable to limits from neutrinoless double beta decay found in Ref. [8], which assume that massive neutrinos are Majorana in nature.

ACKNOWLEDGMENTS

This work was supported by the Natural Sciences and Engineering Research Council of Canada and TRIUMF through a contribution from the National Research Council of Canada and by Research Fund for Doctoral Program of Higher Education of China and was partially supported by KAKENHI (Grants No. 18540274 and No. 21340059) in Japan. M. B. was supported by US National Science Foundation Grant No. Phy-0553611. We are indebted to Brookhaven National Laboratory for the loan of the crystals. We would like to thank the TRIUMF detector, electronics, and DAQ groups for the extensive support. We would like to thank A. de Gouvêa and A. Kobach for providing useful information.

[1] S. Weinberg, Phys. Rev. Lett. **19**, 1264 (1967).
[2] See and e.g., A. de Gouvêa, Annu. Rev. Nucl. Part. Sci. **66**, 197 (2016).
[3] M. Gell-Mann, P. Ramond, R. Slansky, in *Supergravity*, edited by P. van Nieuwenhuizen, and D. Z. Freedman (North-Holland, Amsterdam, 1979), p. 315.
[4] A. Boyarsky, O. Ruchayskiy, and M. Shaposhnikov, Annu. Rev. Nucl. Part. Sci. **59**, 191 (2009).
[5] T. Asaka, S. Eijima, and H. Ishida, J. High Energy Phys. 04 (2011) 011.
[6] B. Bertoni, S. Ipek, D. McKeen, and A. Nelson, J. High Energy Phys. 04 (2015) 170.
[7] B. Batell, T. Han, D. McKeen, and B. Haghi, arXiv: 1709.07001.
[8] A. de Gouvêa and A. Kobach, Phys. Rev. D **93**, 033005 (2016).
[9] R. E. Shrock, Phys. Rev. D **24**, 1232 (1981); See also T. Appelquist, M. Piai, and R. Shrock, Phys. Rev. D **69**, 015002 (2004).
[10] C. Patrignani *et al.* (Particle Data Group Collaboration), Chin. Phys. C **40**, 100001 (2016) and 2017 update.
[11] D. I. Britton *et al.*, Phys. Rev. Lett. **68**, 3000 (1992); Phys. Rev. D **49**, 28 (1994).
[12] G. Czapek *et al.*, Phys. Rev. Lett. **70**, 17 (1993).
[13] A. Aguilar-Arevalo *et al.*, Phys. Rev. Lett. **115**, 071801 (2015).
[14] W. J. Marciano and A. Sirlin, Phys. Rev. Lett. **71**, 3629 (1993).
[15] M. Finkemeier, Phys. Lett. B **387**, 391 (1996).
[16] V. Cirigliano and I. Rosell, J. High Energy Phys. 10 (2007) 005.
[17] N. de Leener-Rosier *et al.*, Phys. Lett. B **177**, 228 (1986).
[18] D. I. Britton *et al.*, Phys. Rev. D **46**, R885 (1992).
[19] M. Aoki *et al.*, Phys. Rev. D **84**, 052002 (2011).
[20] A. Aguilar-Arevalo *et al.*, Nucl. Instrum. Methods Phys. Res., Sect. A **609**, 102 (2009).
[21] A. Aguilar-Arevalo *et al.*, Nucl. Instrum. Methods Phys. Res., Sect. A **791**, 38 (2015).
[22] A. Aguilar-Arevalo *et al.*, Nucl. Instrum. Methods Phys. Res., Sect. A **621**, 188 (2010).
[23] See Supplemental Material http://link.aps.org/supplemental/10.1103/PhysRevD.97.072012 for numerical values of the upper limits on $|U_{ei}|^2$.